



CrossMark
click for updates

Cite this: *RSC Adv.*, 2016, 6, 98682

Fuchsine biosorption using *Asplenium nidus* biosorbent—a mechanism using kinetic and isotherm data

Dissanayake D. M. R. E. A.,^{ab} Wijesinghe W. M. K. E. H.,^{ab} Iqbal S. S.,^{*c} Priyantha N.^b and Iqbal M. C. M.^a

Textile dye contamination of waterways is a major environmental and health issue related to small and medium size enterprises in developing countries. Conventional decontamination techniques are expensive for these enterprises. Biosorption is cost effective, simple and an efficient method for decontamination. An understanding of the adsorption mechanism under optimum reaction conditions would enable the efficient utilization of the biosorbent. We determined the adsorption behaviour of a biosorbent prepared from the ornamental fern *A. nidus* and fuchsine dye under different experimental parameters. Kinetic data were fitted to adsorption kinetic models and adsorption diffusion models. Isotherm data were fitted to two-parameter and three-parameter isotherm models. This paper postulates a mechanism for the adsorption of fuchsine dye onto the biosorbent using kinetic, isotherm and thermodynamic data. The biosorbent adsorbed 88% of fuchsine after 150 min, under the experimental conditions. The adsorption percentage increased when the biomass dose was increased from 0.1 g to 0.2 g and remained the same thereafter. Kinetic data showed that the pseudo second order kinetic model is more applicable and both intraparticle diffusion and liquid film diffusion control the rate of the adsorption process. Isotherm studies showed that the Langmuir–Freundlich isotherm model explains the adsorption process well with a maximum adsorption capacity of 12.95 mg g⁻¹ of dry biosorbent. Thermodynamic parameters suggest that the adsorption is a spontaneous exothermic process with an enthalpy change of -59.26 kJ mol⁻¹ and entropy change of -0.09 kJ mol⁻¹ K⁻¹. It can be concluded that the adsorption is governed by diffusion through the liquid film and within the biosorbent particle surface forming covalent and hydrogen bonding interactions between fuchsine molecules and functional groups of the adsorbent and π - π electron interactions between phenyl rings of the dye molecule.

Received 27th July 2016
Accepted 10th October 2016

DOI: 10.1039/c6ra19011a

www.rsc.org/advances

1 Introduction

Water pollution due to textile dye waste is a major problem associated with small and medium-sized enterprises in developing countries. Due to a lack of financial resources, most small scale textile industries do not invest in expensive decontamination processes; they discharge their effluents into nearby water streams without pre-treatment. Colour is a major determinant of public preference for potable water, and discharge of textile dye waste into nearby water streams is a cause of concern. Beside their colour, textile dyes are also a health hazard since they can cause mutations, chronic health problems such as cancers and birth defects in humans and other life forms.

Textile dyes are categorized according to their chemical nature as acidic, basic and neutral.¹ More often, dyes which are used in textile industries are synthetic. They are therefore stable in chemical environments, and to light, high heat and oxidation, and hence are difficult to biodegrade.

Fuchsine is a magenta coloured triphenylmethane dye² in aqueous medium and commercially available as dark green crystals. An aqueous solution of fuchsine shows basic characters due to the presence of amino groups, whereas it shows acidic characteristics upon modification with sulfonic groups. Fuchsine dye is carcinogenic to humans, and the International Agency for Research on Cancer (IARC) has listed it under IARC group 2B as a possible carcinogen.³ This triphenylmethane dye is extensively used in textile, paper printing and the cosmetic industry due to its low cost and effectiveness.⁴ Excessive use of fuchsine dye leads to contamination of the environment through discharge of wastewater and solid waste. Particulate matter of fuchsine is known to cause respiratory disorders,⁵

^aPlant Biology Laboratory, National Institute of Fundamental Studies, Hanthana Road Kandy, Sri Lanka

^bPostgraduate Institute of Science, University of Peradeniya, Peradeniya, Sri Lanka

^cFaculty of Natural Sciences, Open University of Sri Lanka, Nawala, Sri Lanka. E-mail: ssiqb@ou.ac.lk; Fax: +94 812 232 131; Tel: +94 812 232 002

such as irritations of the nose² and prolonged contamination can cause bladder tumours.^{6,7}

Decontamination of this dye from the aqueous environment by utilizing chemical methods is highly costly, and further, accumulation of toxic sludge creates disposal problems. Physical methods utilize adsorption mechanisms and membrane filtration methods.^{8,9} Physical methods are widely used due to their flexibility, simple operation and more importantly, they do not produce any harmful waste materials. Nevertheless, it is limited due to its initial cost and limited life time of filters used in the membrane filtration process.⁸ On the other hand, utilization of microbial biomass, such as fungi and bacteria, is economically friendly.¹⁰ Therefore, a combination of biological treatment and adsorption on to effective adsorbents, such as activated carbon, has become attractive, although the widespread use of activated carbon alone is limited due to high cost.⁸

Due to these limitations, there is a high demand for low-cost adsorbents for dye removal, where the liquid-phase adsorption is a popular method for removal of pollutants from wastewater. Many mechanisms are involved in adsorption, which depends on the surface chemistry, surface charge and pore structure of the adsorbent, and interactions between adsorption surface and synthetic dye molecules, such as electrostatic and non-electrostatic (hydrophobic) interactions, chelating and complexing interactions and ion exchange due to surface ionization.^{8,11,12}

In this research, *Asplenium nidus* L., an ornamental epiphytic fern, indigenous to Hawaii and Africa, was used as a biosorbent. These ferns grow in elevations up to 760 m.¹³ It is a rosette shaped fern with all of the fronds growing from a central area. The fronds are undivided and sword-shaped. They can be 60 to 120 cm long and 7 to 20 cm wide. They are light green with a dark brown or black midrib.^{13,14}

This research illustrates how fuchsine dye is adsorbed on to the biosorbent prepared from *A. nidus* under different experimental conditions, such as contact time, pH and initial dye concentrations. Data obtained from these experiments were fitted to different kinetic models and isotherm models to understand the adsorption mechanism of fuchsine dye on to the biosorbent. Further, understanding of the adsorption process would provide essential information to postulate an adsorption mechanism, and thereby to further improve the adsorption process to apply in practice.

2 Materials and methods

2.1 Biosorbent preparation

Fresh leaves of *A. nidus* were collected from domestic gardens. The leaves were washed with tap water followed by deionized water. The plant species was identified by comparing with an authenticated sample in the National Herbarium, Sri Lanka. Thoroughly washed leaves were air dried for 48 h and oven dried at 80 °C for 48 h. The biosorbent was prepared by grinding the dried fern leaves and sieving to obtain a particle size fraction between 250 µm and 350 µm. The biosorbent was stored in plastic containers until use. Experiments were conducted in triplicate.

2.2 Chemicals and instrumentation

All the chemicals used were of analytical grade from BDH Chemicals, England and Sigma Aldrich Chemicals, USA. Standard dye solutions of fuchsine (C₂₀H₁₉N₃·HCl) were prepared in deionized distilled water. The initial pH of the working solutions was adjusted using either nitric acid (HNO₃) or sodium hydroxide (NaOH).

The fuchsine dye concentrations were determined using a UV-Visible spectrophotometer (Shimadzu model no. UV-VIS 2450) at the wavelength of 543 nm. The pH of solutions was determined using Hatch Hd 30Q portable pH meter. Fourier transform infrared (FTIR) spectra of the native and dye-loaded samples were obtained from FTIR spectrophotometer (Thermo Science Model NICOLET 6700). The sample disks were prepared using anhydrous KBr and the spectral range was from 4000 cm⁻¹ to 400 cm⁻¹. Biosorbent-dye suspensions were shaken on an orbital shaker (Gallenkamp). Scanning electron microscopic (SEM) images were obtained using ZEISS EVO LS15.

2.3 Characterization of the biosorbent

2.3.1 Determination of the surface area and the surface charge of the biosorbent. The specific surface area of the biosorbent was determined by the methylene blue adsorption method. For this purpose, a series of methylene blue solutions of concentration from 2.0×10^{-6} to 5.0×10^{-6} mol L⁻¹ was prepared; 50 mg of the biosorbent was suspended in each solution and shaken gently for 3.0 h to ensure that adsorption equilibrium was reached. Suspensions were centrifuged and the supernatants were analysed for the remaining methylene blue concentration by UV-visible spectrophotometry at the wavelength of 665 nm. The dry biosorbent (1.0 g) was suspended in 100 mL of 0.1 mol L⁻¹ NaNO₃ solution in a sealed vessel and N₂ gas was bubbled through the suspension while stirring at a constant rate for 3.0 h to remove dissolved CO₂. Thereafter, stirring was continued for another 12.0 h in a CO₂ free environment to obtain a homogeneous solution. The initial pH of the suspension was measured and the pH was adjusted to 10.0 by adding a concentrated solution of NaOH. The mixture was then titrated by adding small aliquots of HNO₃ solution of known concentration until the pH of 3.0 was reached, and the pH was then measured after each addition. The system was continuously and steadily stirred and purged with N₂ throughout the titration. A back titration was carried out using the same NaOH solution and a blank titration was conducted in the absence of the biosorbent. The entire procedure was repeated for two more ionic strengths (0.01 mol L⁻¹ and 0.001 mol L⁻¹).

2.3.2 Characterization of the biosorbent surface and surface functional groups. The functional groups on the biosorbent surface were determined using FTIR spectral analysis. Spectral data were obtained for the native biosorbent and fuchsine-adsorbed biosorbent. For the preparation of FTIR sample disks, finely ground biosorbent was thoroughly mixed with analytical grade potassium bromide (KBr). The sample disks were stored in a desiccator for 48 h, and the FTIR spectra were obtained in the wave number range 400–4000 cm⁻¹.

2.4 Study of experimental parameters on biosorption

Suspensions of biosorbent (0.200 g) in 100.0 mL each of 5.0 mg L⁻¹ fuchsine dye solution at pH 5.0 were shaken at a speed of 100 rpm. The contents were removed at predetermined time intervals, filtered and the filtrate was analysed for residual dye content. To determine the effect of biosorbent dosage on biosorption, the experiment was repeated using 0.100 g and 0.400 g of the biosorbent. The same experiment was repeated by varying the initial solution pH in the range 1.0 to 10.0 to determine the effect of initial pH. Fuchsine dye solutions whose concentration varied from 1.0 mg L⁻¹ to 15.0 mg L⁻¹ at pH 5.0 were used to determine the effect of initial dye concentration on biosorption. All the experiments were conducted at an ambient temperature of 27 °C.

3 Analysis of batch adsorption data

The percentage of adsorption (A%) was calculated using equation:

$$A\% = \frac{(C_i - C_f)}{C_i} \times 100 \quad (1)$$

and the adsorption amount (q) was calculated using equation:

$$q = \frac{(C_i - C_f)}{M} V \quad (2)$$

where C_i and C_f are the initial and final dye concentrations (mg L⁻¹) respectively, of the solution, which were determined using absorbance data. V (L) is the volume of fuchsine solution and M (mg) is the amount of biomass used.

3.1 Kinetics and isotherm modelling

Kinetic and isotherm modelling of the biosorption process is used to understand the mechanism of the biosorption process. Successful implementation of the adsorption system would depend on the mechanism. In this study, the data were fitted to four kinetic models and four isotherm models to understand the adsorption of fuchsine on to the biosorbent.

3.1.1 Adsorption kinetic models

3.1.1.1 Pseudo first and pseudo second order kinetics. Most fundamental models used in kinetics modelling are pseudo first order (eqn (3)) and pseudo second order (eqn (4)) models. These kinetic models illustrate the relationship between the adsorbent and the adsorbate. In this study, non-linear pseudo first order and pseudo second order kinetic models were used to determine the order of the adsorption process. Linear forms of the equations are given by eqn (3-b) and (4-b) respectively.

$$q_t = q_e(1 - \exp^{-k_1 t}) \quad (3)$$

$$\ln(q_e - q_t) = \ln q_e - \ln k_1 t \quad (3-b)$$

$$q_t = \frac{k_2 q_e^2 t}{1 + k_2 q_e t} \quad (4)$$

$$1/q_t = 1/(k_2 q_e^2 t) + 1/q_e \quad (4-b)$$

where q_e and q_t denote the amounts of fuchsine ions adsorbed per unit mass of the sorbent (mg g⁻¹ dry biomass) at equilibrium and at time t , respectively, k_1 and k_2 are the pseudo-first order rate constant (min⁻¹) and the pseudo-second-order rate constant (g mg⁻¹ min⁻¹), respectively. The amount of fuchsine adsorbed on to the biosorbent was calculated using eqn (2).^{15,16}

3.1.2 Adsorption diffusion models

3.1.2.1 Intraparticle diffusion and liquid film diffusion model. Intraparticle diffusion model and the liquid film diffusion model were used to understand the interaction between the adsorbate and the adsorbent. Behaviour of the adsorption data with regard to intraparticle diffusion models and film diffusion mass transfer model were determined using equation:

$$q_t = k_{\text{int}} t^{0.5} \quad (5)$$

where k_{int} is the intraparticle diffusion constant, and equation:

$$\ln\left(1 - \frac{q_t}{q_e}\right) = -R^1 t \quad (6)$$

where, R^1 is the liquid film diffusion constant (min⁻¹), given by $\left[R^1 = \frac{3D_e^1}{r_0 \Delta r_0 k^1}\right]$ where, D_e^1 is the effective liquid film diffusion coefficient (cm² min⁻¹), r_0 is the radius of the adsorbent particle (cm), Δr_0 is the thickness of the liquid film (cm) and k^1 is the equilibrium constant of adsorption.¹⁶

3.1.3 Two parameter isotherm models

3.1.3.1 Langmuir isotherm. The Langmuir isotherm describes the formation of a monolayer of fuchsine on the biosorbent surface. The model is only valid for monolayer adsorption. The Langmuir isotherm model is given by equation:

$$q_e = \frac{q_0 b C_e}{1 + b C_e} \quad (7)$$

$$1/q_e = 1/q_0 + 1/bq_0 C_e \quad (7-b)$$

where q_e is the amount of fuchsine adsorbed per unit mass of the biosorbent (mg g⁻¹) at equilibrium, b is the adsorption coefficient, q_0 is the amount of fuchsine adsorbed per unit mass of the biosorbent (mg g⁻¹) (*i.e.* monolayer saturation capacity) and C_e is the residual fuchsine concentration (mg L⁻¹) at equilibrium. The values of b and q_0 were evaluated from a plot of q_e vs. C_e .¹⁷

The adsorption intensity, R_L , for the Langmuir isotherm was calculated using equation:

$$R_L = 1/(1 + b C_i) \quad (8)$$

which has four probabilities: (1) $0 < R_L < 1$, favourable adsorption; (2) $R_L > 1$, unfavourable adsorption; (3) $R_L = 1$, linear adsorption; and (4) $R_L = 0$, irreversible adsorption.¹⁸

3.1.3.2 Freundlich isotherm model. The Freundlich isotherm describes the formation of multilayers of the adsorbate on the heterogeneous biosorbent surface, given by the equation:

$$q_e = k_f C_e^{1/n} \quad (9)$$

$$\ln q_e = \ln k_f + 1/n \ln C_e \quad (9-b)$$

where k_f and n are the constants related to adsorption capacity and adsorption intensity, respectively. These constants were determined from a plot of q_e vs. C_e .^{17,19}

3.1.3.3 Dubinin–Radushkevich model. The Dubinin–Radushkevich isotherm model expresses the adsorption mechanism with Gaussian energy distribution. From this model, the nature of the adsorption process can be determined. This model is given by equation:

$$q_e = q_0 \exp\left\{-\left[\frac{RT \ln(C_s/C_e)}{E}\right]^2\right\} \quad (10)$$

$$\ln q_e = \ln q_0 - \left[\frac{RT \ln(C_s/C_e)}{E}\right]^2 \quad (10-b)$$

where R is the universal gas constant, T is the absolute temperature (K), C_s is the saturation concentration of fuchsin and $\left[E = \left[\frac{1}{\sqrt{2\beta}}\right]\right]$ is the mean free energy per molecule of adsorbent where β is the Dubinin–Radushkevich constant ($\text{mol}^2 \text{J}^{-2}$) and is determined by the plot of q_e vs. C_e .¹⁹

3.1.4 Three parameter isotherm models

3.1.4.1 Langmuir–Freundlich isotherm model. The combined Langmuir–Freundlich isotherm explains both Langmuir and Freundlich behaviours. It follows the Freundlich isotherm at low adsorbate concentration and the Langmuir isotherm at high adsorbate concentrations.¹⁷ The Langmuir–Freundlich isotherm is given by:

$$q_e = \frac{q_0(k_a C_e)^n}{(k_a C_e)^n + 1} \quad (11)$$

where k_a is the affinity constant for adsorption (L mg^{-1}) and n is the index of heterogeneity. The values of k_a , q_0 and n were evaluated using the plot of q_e vs. C_e .²⁰

3.1.4.2 Redlich–Peterson isotherm model. This is also a hybrid of the Langmuir and Freundlich models. This model can predict the behaviour of the adsorption system with linear dependence and the exponential dependence of the adsorbate concentration.^{21,22} Due to the linear and exponential dependency of the model, it can be used to cover a wide range of concentrations. The Redlich–Peterson model is given by:

$$q_e = \frac{k_{\text{RP}} C_e}{1 + a_{\text{RP}} C_e^{\beta_1}} \quad (12)$$

$$\ln(k_{\text{RP}} C_e^{\beta_1} q_e - 1) = \beta_1 \ln(C_e) + \ln a_{\text{RP}} \quad (12-b)$$

where, k_{RP} is the affinity constant for adsorption (L mg^{-1}), a_{RP} is the Redlich–Peterson isotherm constant (mg^{-1}) and β_1 is the index of heterogeneity.^{17,23}

3.2 Thermodynamic study

The thermodynamic parameters of the adsorption process were calculated at 27 °C, 35 °C, 40 °C, 45 °C and 50 °C using

Langmuir isotherm data. Gibbs free energy change (ΔG) of the adsorption process is given by,

$$\Delta G = -RT \ln b \quad (13)$$

where, R is the universal gas constant, T is the absolute temperature (K), and b is the Langmuir constant.⁷

The relationship between Gibbs free energy change ΔG , the enthalpy change ΔH , and the entropy change ΔS is given by eqn (14).

$$\Delta G = \Delta H - T\Delta S \quad (14)$$

The intercept of the plot of ΔG vs. T will give the enthalpy change (ΔH) and the slope of the plot will result in the entropy change (ΔS) of the adsorption system.^{9,24}

4 Results and discussion

4.1 Characterization of the biosorbent

4.1.1 Surface area and the surface charge of the biosorbent.

The average amount of methylene blue adsorbed on the biosorbent surface at equilibrium was 2.5×10^{-7} mol. The specific surface area determined by eqn (15) was $3.99 \text{ m}^2 \text{ g}^{-1}$.

$$s = M_{\text{mb}} \times N_A \times A_{\text{mb}}/m \quad (15)$$

where M_{mb} is the amount of methylene blue adsorbed (mol) for the completion of the monolayer, A_{mb} is the surface area of the methylene blue molecule (130 \AA^2), m is the amount of biosorbent in the suspension (g), and N_A is the Avogadro constant (6.022×10^{23}).²⁵

The surface charge (σ) of the biosorbent was determined by the equation:

$$\sigma = \{[F(a \times s)]\} \{(C_a - C_b) - [H^+] + [OH^-]\} \quad (16)$$

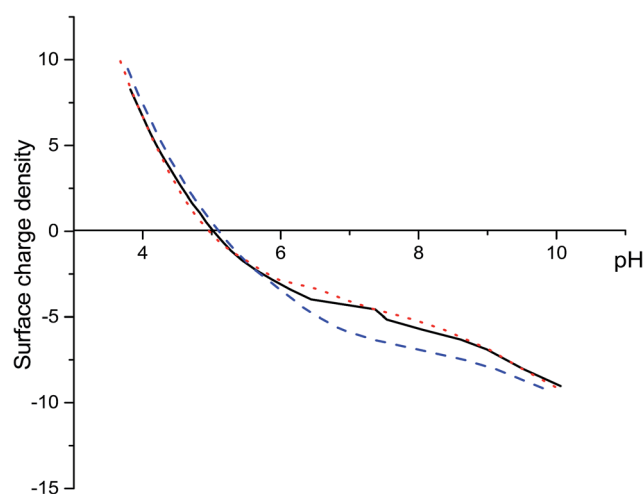


Fig. 1 Variation of surface charge density of *A. nidus* biosorbent with solution pH at different ionic strengths (— 0.001 mol L⁻¹, - - - 0.01 mol L⁻¹, 0.1 mol L⁻¹).

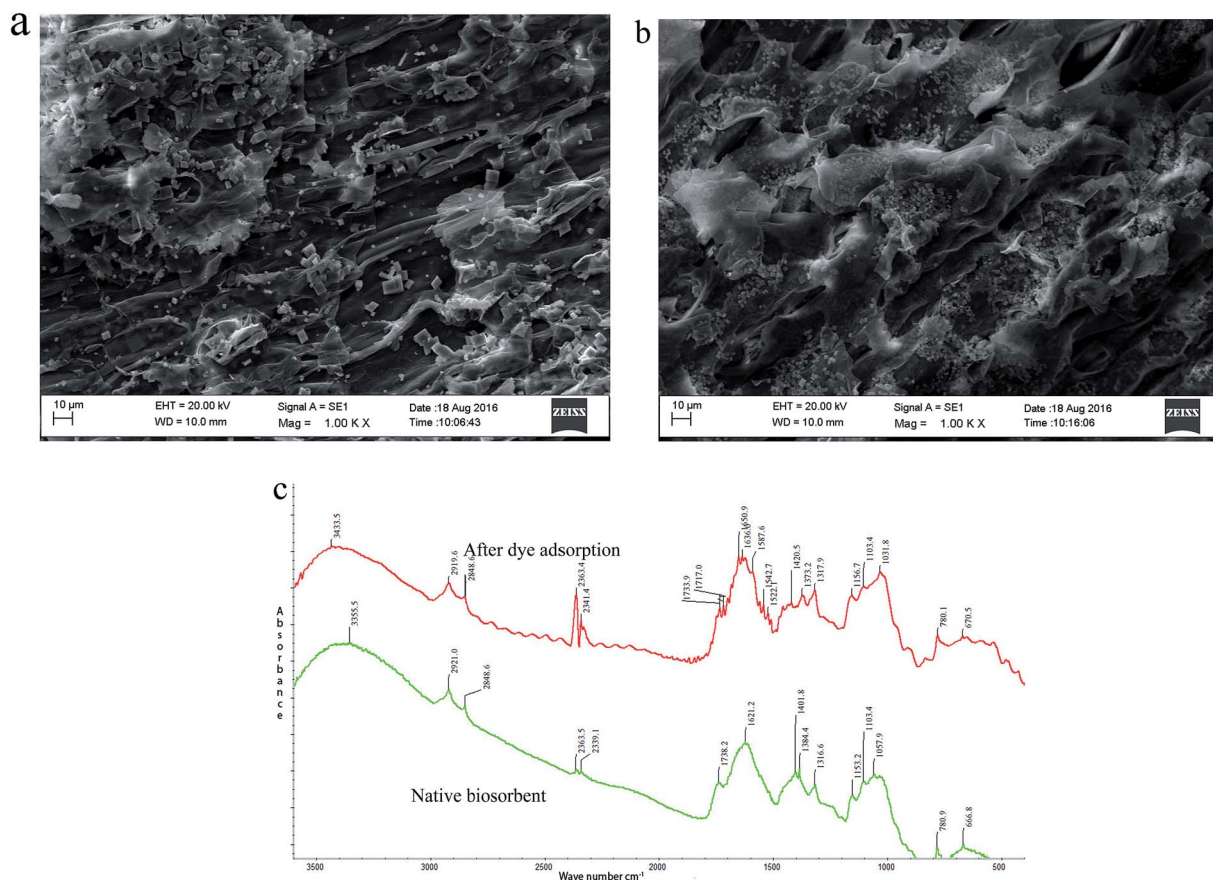


Fig. 2 Scanning electron microscope images of the native biosorbent (a) and the dye adsorbed biosorbent (b); (c) FT-IR spectrum of native and dye adsorbed *A. nidus* biosorbent.

where F is the Faraday constant, a is the mass of the biosorbent in the suspension (1.00 g), s is the surface area of the biosorbent ($3.99 \text{ m}^2 \text{ g}^{-1}$), C_a and C_b are the calculated concentrations (mol L^{-1}) of the acid and the base, respectively, in the medium at a particular point of titration. $[\text{H}^+]$ and $[\text{OH}^-]$ are the hydrogen and hydroxyl ion concentration in the medium according to re-measured pH value at a particular point.^{26,27}

The pH of the medium determines the surface charge of the biosorbent which is calculated by the number of H^+ ions bound to the biosorbent surface during the titration.²⁸ At low pH values, the biosorbent surface was positively charged, which after pH 5.0 became negatively charged for all the ionic strengths tested (Fig. 1). Further, surface charge vs. pH curves for all the ionic strengths intersected at a common point (isoelectric point) of pH 5.5.

4.1.2 Characterization of the biosorbent surface and surface functional groups. Morphology of the biosorbent was studied using scanning electron microscopy before and after dye adsorption. It was observed that the biosorbent surface has a complex structure with irregular and heterogeneous cube like structures (Fig. 2a). When the dye is adsorbed on to the biosorbent surface, it is more homogenous and smooth (Fig. 2b). Functional groups of the biosorbent surface that are responsible for the adsorption were determined by considering the frequency shift of the functional groups before and after the dye

adsorption (Fig. 2c). The FTIR spectrum of native biosorbent shows many vibrational bands indicating that surface of the biosorbent contains several functional groups such as bonded hydroxyl groups ($-\text{OH}$, 3355 cm^{-1}), alcohol groups ($\text{C}-\text{OH}$, 1103 cm^{-1}), alkyl amide groups (1621 cm^{-1}) and carboxylic acid groups (1738 cm^{-1}).^{29–31} It was observed that the peak positions corresponding to carboxylic acid group has shifted to 1717 cm^{-1} (Fig. 2c) indicating its involvement in the dye adsorption. It is also apparent that the biosorbent after the dye adsorption showed sharp absorbance peaks at $1587\text{--}1522 \text{ cm}^{-1}$ (aromatic ring stretch)³⁰ and $1650\text{--}1639 \text{ cm}^{-1}$ (secondary amine)²⁹ which can be related to the functional groups of the fuchsine molecule.

4.2 Effect of contact time on adsorption

The duration of contact between the dye and the biosorbent and the biosorbent dosage were important determinants of bio-sorption of fuchsine. The adsorption of fuchsine dye increased with increase in time to a maximum of 88% after 150 min and remained constant thereafter (Fig. 3). The adsorption was 77% with 0.10 g of biosorbent. Increase in the amount of the biosorbent to 0.20 g and 0.40 g, did not lead to a significant increase in biosorption (Fig. 3). However, the optimum contact time for 0.4 g decreased to 60 min. Since 0.20 g was selected as

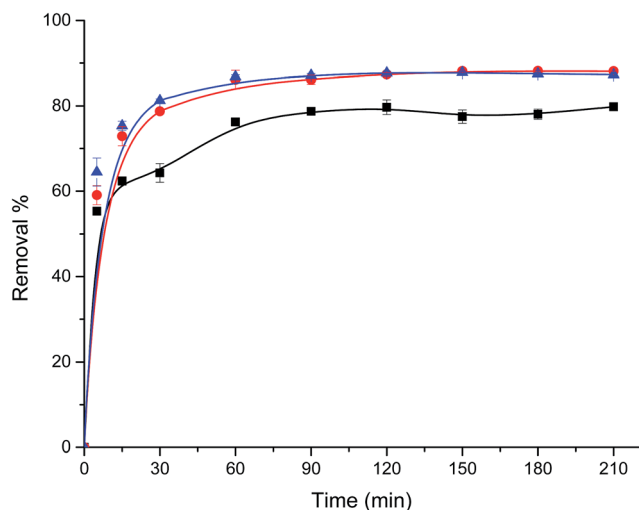


Fig. 3 Percentage removal of fuchsine by *A. nidus* biosorbent at different shaking times (initial dye concentration = 5.0 mg L⁻¹, pH = 5.0, temperature = 27 °C shaking speed = 100 rpm, numbers of replicates (*n*) = 3, ■ 0.1 g, ● 0.2 g, ▲ 0.4 g).

the optimum amount of biosorbent, 150 min was selected as the optimum contact time for further experiments.

The availability of vacant sites on the biosorbent surface determines the rate of biosorption. At the initial stage of the adsorption process, the concentration of the dye and the available vacant sites are high which result in a rapid adsorption of dye molecules on the biosorbent surface.^{11,32} Adsorption of dye molecules on the biosorbent surface involves physisorption and chemisorption processes, where the π electron cloud of the dye interacts with the charged surface of the biosorbent and the positively charged C=NH₂⁺ group of the dye molecule interacts with the functional groups on the biosorbent surface. When the amount of the biosorbent in the system was

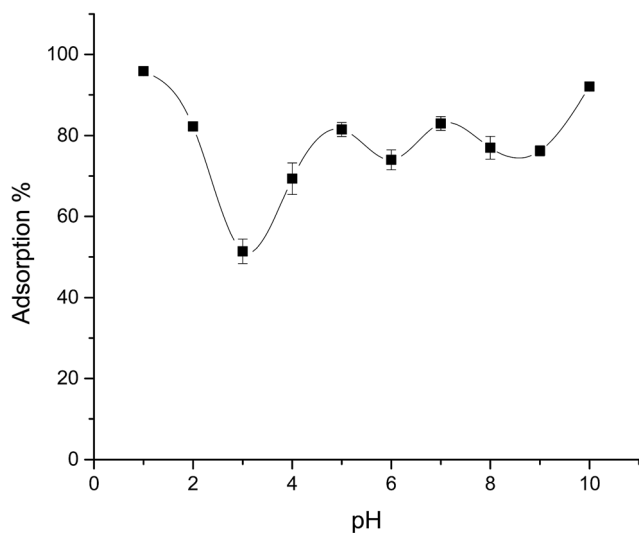


Fig. 4 Effect of pH on biosorption of fuchsine by 0.20 g of *A. nidus* biosorbent (initial dye concentration = 5.0 mg L⁻¹, temperature = 27 °C, shaking speed 100 rpm, *n* = 3).

increased, the rate of adsorption also increased and the time to reach equilibrium was reduced. Similar observations were reported for fuchsine adsorption on to bottom ash and deoiled soya by Gupta *et al.*⁷

4.3 Effect of initial solution pH

The initial solution pH determines the degree of protonation of the adsorbent and the chemical environment, thereby affecting its adsorption capacity. When the pH of the system was extremely low (pH 1–2) or high (pH 10), UV-Visible data showed that the residual dye concentration was 10–20% of the initial dye concentration (Fig. 4). This could probably be due to the structural changes of the dye at extreme pH values and hence absorbance at 543 nm of fuchsine dyes was reduced and maximum adsorption shifted towards 300 nm. At low pH (pH 3–4), the biosorbent surface is positively charged,³³ which would electrostatically repel positively charged C=NH₂⁺, but attract the π electron clouds of the phenyl groups in the fuchsine dye molecule showing a moderate adsorption of the dye of 50–60%. Low initial pH of the solution can also damage the biosorbent structure, affecting its adsorption capacity.³⁴ The optimum pH of 5–9, enabled maximum adsorption of 88% of fuchsine (Fig. 4). Similar observations were reported for fuchsine adsorption on bottom ash and deoiled soya⁷ and malachite green adsorption on rice husk-based active carbon.¹¹

4.4 Adsorption kinetic models

4.4.1 Kinetics of the adsorption process. Understanding the kinetics of the biosorption process is useful to predict the mechanism of adsorption and to design practical applications. The values of the rate constants k_1 and k_2 , and q_e obtained for each model are presented in Table 1. There was a noticeable difference in the R^2 values for each model (Table 1), and the q_e value predicted by the pseudo second order kinetic model was closer to the experimental q_e value than the q_e value predicted by the pseudo first order model. Considering both factors (R^2 and q_e), it is reasonable to assume that the adsorption process follows pseudo second order kinetics. The rate constant k_2 of the pseudo second order kinetics increased with the increase in biosorbent dosage (Table 1). Therefore this can imply that the rate of adsorption is proportional to the number of active sites on the biosorbent.³⁵ Biosorption is a multi-step sorption process that involves an initial rapid phase of diffusion and the later slower phase of exchange or sharing of electrons between the fuchsine molecule and the biosorbent surface until the saturation of the biosorbent.³⁶ Similar explanations have been reported based on the observation for fuchsine adsorption on to bottom ash and deoiled soya,⁷ and removal of Pb²⁺ from an aqueous solution using a non-living moss biomass.³⁷

4.4.2 Adsorption diffusion models. In biosorption, the rate of adsorption is determined by intraparticle diffusion or liquid film diffusion. Depending on the nature of adsorption, the rate-determining step would change. If the process is physical, the rate of adsorption will be determined by the liquid film diffusion or intraparticle diffusion. If the process is chemical then the rate-controlling step will be the mass transfer from the bulk

Table 1 Parameters calculated for different kinetic models for biosorption of fuchsine on *A. nidus* biosorbent (initial dye concentration 5.0 mg L⁻¹, initial pH 5.0, shaking speed = 100 rpm, temperature 27 °C, *n* = 3) see text for abbreviations

Biomass (g)	$q_{e(\text{exp})}$	Pseudo 1 st order			Pseudo 2 nd order			Intraparticle diffusion		Liquid film diffusion	
		q_e	k_1	R^2	q_e	k_2	R^2	k_{int}	R^2	R^1	R^2
0.1	3.32	2.5	0.25	0.46	3.34	0.11	0.978	0.13	0.963	-0.02	0.985
0.2	1.85	1.79	0.21	0.973	1.87	0.19	0.997	0.07	0.832	-0.03	0.918
0.4	0.95	0.92	0.26	0.978	0.96	0.5	0.997	0.032	0.843	-0.04	0.948

solution to the surface of the adsorbent to form a chemical bond.¹⁶ The intraparticle diffusion model assumes that diffusion within the particle is the only rate-controlling process where the zero intercept of the plot of q_t vs. $t^{0.5}$ indicates the acceptability of this model. However, the plot of q_t vs. $t^{0.5}$ did not pass through the origin for the three quantities of biomass tested (Fig. 5a), indicating that intraparticle diffusion is not the only rate-controlling mechanism for fuchsine adsorption on to the biosorbent.³¹ The intraparticle diffusion constant (k_{int}) for fuchsine adsorption varied from 0.12 to 0.032 mg g⁻¹ min^{0.5}. The highest k_{int} was for 0.10 g biosorbent, which was the lowest amount used; further, k_{int} decreased when the biosorbent

amount was increased, indicating faster adsorption rates for low biomass values due to more efficient transfer to limited number of adsorption sites. The liquid film diffusion model assumes that the rate of adsorption is dependent on the solute transfer through the liquid film. The plot of the experimental data for the liquid film diffusion model (Fig. 5b) gave a linear relationship for $\ln(1 - q_t/q_e)$ vs. t , with a high correlation coefficient (>0.91, Table 1) and negative gradient. Therefore, it is predicted that the rate limiting step of the adsorption process is liquid film diffusion. Thus the overall kinetics of the adsorption process is controlled initially by transfer of solute (*i.e.*, the dye) to the surface of sorbent particles by liquid film diffusion and transfer from the sorbent surface to the intraparticle active sites. This is followed by adsorption through exchange or sharing of electrons of the dye molecule and the active sites of the biosorbent surface.³⁸

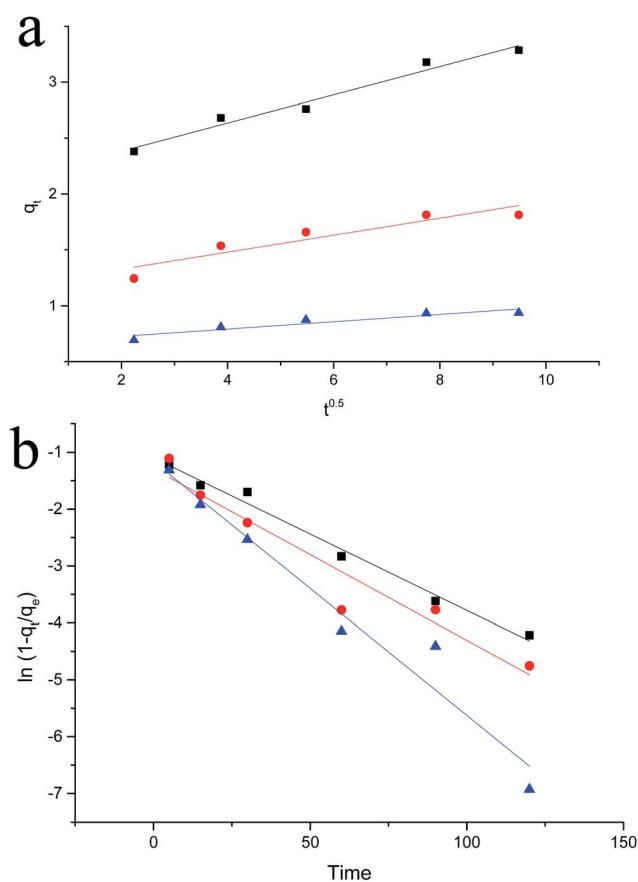


Fig. 5 (a) Intraparticle diffusion model and (b) liquid film diffusion model for fuchsine adsorption on to *A. nidus* biosorbent (initial dye concentration = 5.0 mg L⁻¹, pH = 5.0, temperature = 27 °C, shaking speed = 100 rpm, *n* = 3, ■— 0.1 g, ●— 0.2 g, ▲— 0.4 g).

4.5 Adsorption isotherm models

4.5.1 Two parameter isotherm study. The two parameter isotherm study showed that both Langmuir and Freundlich isotherms are compatible with adsorption of fuchsine on to the biosorbent (Fig. 6) with reasonably high R^2 values of 0.971 and 0.968 (Table 2). Adsorption intensity (R_L) calculated for the

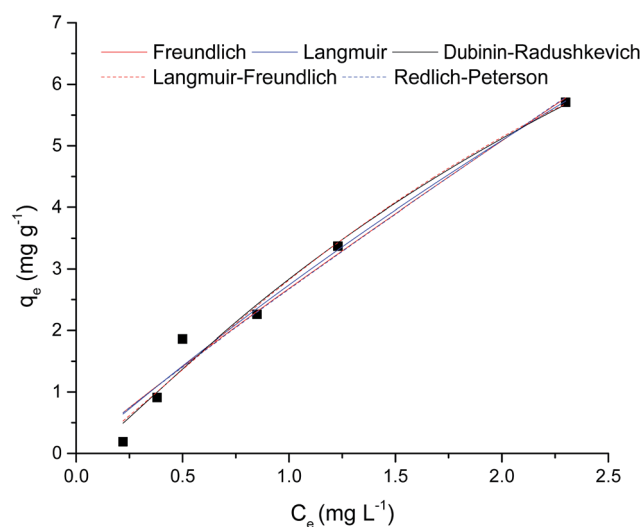


Fig. 6 Isotherm curves for fuchsine adsorption on to 0.20 g of *A. nidus* biosorbent at pH 5.0 at 27 °C temperature (shaking speed 100 rpm, *n* = 3).

Table 2 Adsorption isotherm parameters for fuchsine adsorption on to 0.20 g of *A. nidus* leaves (temperature = 27 °C, pH = 5.0, shaking speed = 100 rpm, $n = 3$). See text for abbreviations^a

Model	k	q_0	N	E	a_{RP}	C_s	R^2
Langmuir	0.08	35.74	NA	NA	NA	NA	0.971
Freundlich	2.68	NA	1.08	NA	NA	NA	0.968
Dubinin–Radushkevich	0.01	14.32	NA	6.68	NA	30.280	0.968
Langmuir–Freundlich	0.35	12.95	1.24	NA	NA	NA	0.966
Redlich–Peterson	2.81	NA	2.48	NA	0.016	NA	0.962

^a NA = not applicable.

Langmuir isotherm varied from 0.47–0.95, indicating that the adsorption process is favourable ($0 < R_L < 1$).¹⁷ The monolayer adsorption capacity (q_0) of the adsorbent determined by the Langmuir isotherm was 35.74 mg g⁻¹, which is equivalent to a monolayer.

The Freundlich isotherm model assumes the formation of multilayer of adsorbate on the heterogeneous adsorbent surface, where heterogeneity of the biosorbent surface or the adsorption intensity is represented by $1/n$. When the surface becomes more heterogeneous, the value of $1/n$ becomes closer to zero.¹⁷ For the adsorption of fuchsine on to the biosorbent, the $1/n$ value was 0.92 (Table 2), indicating that the surface of the biosorbent is less heterogeneous. Further, the Freundlich constant (k_f) for the adsorption process was 2.68 mg g⁻¹. A high k_f value for fuchsine adsorption suggests that the adsorption process is favourable and explains the high percentage adsorption (88%) of dye on to the biosorbent.

Interpretation of experimental data based on Dubinin–Radushkevich isotherm model suggests that the adsorption mechanism is on to a heterogeneous surface. Using this isotherm model, it is possible to distinguish physical adsorption over a chemical adsorption process using Gaussian energy distribution.^{17,39} Biosorption of fuchsine on to the biosorbent showed a low free energy of 6.69 kJ mol⁻¹ (Table 2) indicating that the adsorption is a physical process.^{18,31} Using the Dubinin–Radushkevich model, maximum adsorption capacity (q_0) calculated for adsorption of fuchsine was 14.32 mg g⁻¹. This value shows greater variation from the q_0 values predicted by the Langmuir model. This may be due to the assumptions made during the model postulation, where, the Langmuir model assumes the formation of a monolayer of adsorbate on the homogeneous surface of the adsorbent whereas Dubinin–Radushkevich assumes that the adsorption takes place on a heterogeneous surface.¹⁷

4.5.2 Three-parameter isotherm study. Most adsorption processes are explained by using either the Langmuir isotherm model or the Freundlich isotherm.^{10,40} However, a few isotherm data agreed with both the Langmuir and the Freundlich isotherms. Thus it is difficult to explain their adsorption behaviour using only two parameter isotherm models individually. To explain such behaviours of adsorption systems, the combined isotherm models of Langmuir and Freundlich isotherms is used.^{20,41}

In the Langmuir–Freundlich combined isotherm model, adsorption follows Langmuir isotherm at high adsorbate concentrations whereas at low adsorbate concentrations it follows Freundlich isotherm characteristics. Our observations showed that the adsorption of fuchsine dye on the biosorbent followed the Langmuir–Freundlich combined isotherm model with a high R^2 value (>0.966). The heterogeneity index predicted by the Langmuir–Freundlich combined model was 1.24 (heterogeneity = 0.82) (Table 2), which is closer to the heterogeneity index predicted by the Freundlich isotherm model. Adsorption capacity, q_0 , of 12.95 mg g⁻¹ (Table 2) predicted by the Langmuir–Freundlich isotherm is closer to q_0 predicted by the Dubinin–Radushkevich model than that by the Langmuir model (Table 2). Therefore, these observations suggest that the adsorption process can be explained by the Langmuir–Freundlich isotherm model.

Using the Redlich–Peterson isotherm, the heterogeneity index of the adsorbent surface can also be predicted (Table 2). For the adsorption of fuchsine dye on to the biosorbent the predicted heterogeneity index value of 2.48 (heterogeneity = 0.36) showed greater deviation from the heterogeneity index predicted by both Freundlich isotherm model and Langmuir–Freundlich isotherm. Though the model showed a high R^2 (0.962), the difference in heterogeneity index suggests the unsuitability of the model to describe the interaction between fuchsine dye and the biosorbent surface.

From the data analysed using different isotherm models, it is possible to suggest that the three parameter isotherm models are more appropriate to explain the adsorption of fuchsine dye on to the biosorbent. The adsorption process can be best explained by the Langmuir–Freundlich combined isotherm.

4.6 Thermodynamic study

To understand the adsorption mechanism of the heavy metal onto the biosorbent, it is important to study the thermodynamic parameters of the adsorption system. This will indicate if the adsorption process is exothermic or endothermic or whether the process is spontaneous or not. When the temperature of the adsorption system is increased from 27 °C to 50 °C (300 K to 323 K), the change in Gibbs free energy (ΔG) increased from -29.50 kJ to -27.24 kJ (Table 3). The negative value of ΔG indicates that the adsorption process is spontaneous.^{42,43} An increment of the negative value of ΔG with decreasing temperature implies that high temperature is unfavourable for the adsorption process. This confirms the reduction of the adsorption percentage at higher temperatures. In general if the ΔG is between 0 and -20 kJ

Table 3 Values of thermodynamic parameters of the fuchsine adsorption onto 0.2 g of *A. nidus* at 100 rpm at pH 5

Temperature (K)	Gibbs free energy ΔG (kJ mol ⁻¹)	Enthalpy change ΔH (kJ mol ⁻¹)	Entropy change ΔS (kJ mol ⁻¹ K ⁻¹)
300	-29.50	-59.26	0.09
308	-28.76		
313	-28.08		
318	-27.72		
323	-27.24		

mol^{-1} , adsorption process is physical in nature while if it is between -80 and -400 kJ mol^{-1} , the process is chemisorption. In our study the ΔG value lies between -29.50 kJ and -27.24 kJ suggesting that the adsorption process is mainly due to physisorption while chemisorption is also involved.⁴⁴ This is further supported by the isotherm study in which it was found that adsorption of dye on to biosorbent follows Freundlich–Langmuir combined isotherm. The negative value ($-59.26 \text{ kJ mol}^{-1}$) of enthalpy change (ΔH) (Table 3) shows that the adsorption process is exothermic²⁴ and the negative value ($-0.09 \text{ kJ mol}^{-1} \text{ K}^{-1}$) for entropy change (ΔS) (Table 3) suggests reduction of randomness of the system during the adsorption process.⁴³ A negative value for ΔH confirms the physical nature of the adsorption process, whereas a positive ΔH indicates the chemisorption process.⁴³ In a physisorption system, dye molecules are attached to the biosorbent through relatively weak H bonds, π - π electron cloud interactions and van der Waals forces. When the temperature of such a system is increased, the kinetic energy of the dye molecule will be increased thereby increasing the movement of molecules, thus breaking the weak bonds between dye molecules and the biosorbent surface. Therefore, the dye molecules will remain in the liquid phase rather than in the solid phase, which results in a lower percentage adsorption.

4.7 Proposed mechanism for the adsorption process

From the adsorption isotherm studies, several mechanisms can be postulated for the adsorption of fuchsine dye on to the biosorbent surface. Initially $\text{C}=\text{NH}$ interacts with functional groups ($\text{R}-\text{OH}$, $\text{R}-\text{COOH}$ and $\text{R}-\text{NH}_2$) on the biosorbent surface and forms hydrogen bonds and covalent bonds (Fig. 7a).⁴⁵ When the concentration increases, more dye molecules arrange to form a layer of dye molecules on the

surface of the biosorbent.^{45,46} These adsorbed dye molecules can act as new hydrogen bond sites for incoming dye molecules and form hydrogen bonding interactions (Fig. 7b). This process will reduce the free energy of adsorption, making the adsorption process favourable. This postulation can be used to describe the predictions made using the Dubinin–Radushkevich isotherm model for Gaussian energy distribution. At high concentrations, the new incoming dye molecules can form π - π electron interactions with the phenyl rings of the dye.⁴⁷ Further, interaction can take place between the amine groups and the π electron cloud of the dye molecules.⁴⁸ Therefore, it is suggested that the adsorption of fuchsine on to the biosorbent surface is a complex process, which includes liquid film diffusion and intraparticle diffusion of dye on to the biosorbent surface and covalent bonding interaction, hydrogen bonding interaction between fuchsine molecules and functional groups of the adsorbent and π - π electron interactions between phenyl rings of the dye. Similarly benzene rings of the fuchsine molecule can interact with the functional groups on the biosorbent surface through van der Waals forces and electrostatic interaction between atoms.⁴⁹

4.8 Significance of the present study

The high adsorption capacity (q_m) given in Table 4 is for adsorbents prepared by physical modification to very small particle size distribution of activated carbon and in some cases followed by chemical treatment. However, although the adsorption capacities were high, the percentage removal is similar to that in our study. High adsorption capacity may be due to the smaller particle size, which increases the surface area of the adsorbent. In our study we used the biosorbent of

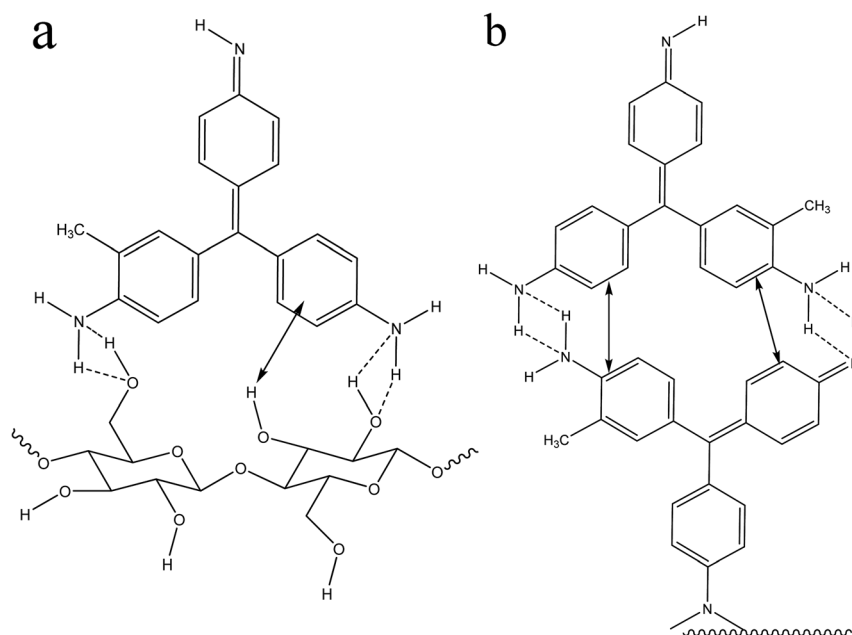


Fig. 7 Schemes of the (a) proposed interactions between biosorbent (cellulose) and the fuchsine dye (b) formation of multi layers during the adsorption process. (\leftrightarrow π electron interactions, $-$ hydrogen bonds).

Table 4 Comparison of the adsorption capacity with literature data^a

Adsorbent	Particle size mm	Concentration range	Q_{\max}	Percentage	Reference
Cation-exchange resin		25–700 ^a	127.0 ^c	18–74%	50
Bottom ash	0.08–0.425	$1-8 \times 10^{-5b}$	2.12 ^d	83.75–89%	7
Deoiled soya	0.08–0.300		3.99 ^d	94.25–98%	
<i>Zizania latifolia</i> AC	0.074–0.105	200 ^a	135 ^c	Not given	5
<i>Zizania latifolia</i> AC Fe(III) modified			212.77 ^c		
<i>Zizania latifolia</i> AC Mn(II) modified			238.10 ^c		
Leather waste AC	0.149–0.105		132–139 ^c	>90%	51
Leather waste AC-Mn(II) modified			130–182 ^c		
<i>A. nidus</i>	0.250–0.350	1–15 ^a	12.95 ^c	88%	Present study

^a AC = activated carbon a = mg L⁻¹, b = mol L⁻¹, c = mg g⁻¹, d = mol g⁻¹.

moderate range of particle size without modification which implied less preparation cost. The adsorbent with moderate particle size range has the advantages that it will not cause turbidity in the water since it can be easily filtered.

5 Conclusions

The present study demonstrated that the biosorbent prepared from the *A. nidus* leaves can be successfully used as adsorbents to remove fuchsine dye from the aqueous environment. The maximum adsorption occurred in the region of pH 4–9. The kinetics of adsorption followed the pseudo-second kinetic model and both intraparticle diffusion and liquid film transfer control the rate of adsorption. Equilibrium data for fuchsine adsorption adequately follow the combined Langmuir–Freundlich isotherm model. Adsorption of fuchsine on to the biosorbent surface is a complex process where, fuchsine molecules diffuse through the liquid film on to the biosorbent surface. Thereafter it is transferred to the functional groups on the biosorbent surface through intraparticle diffusion. After diffusion, covalent bonding interaction, hydrogen bonding interaction between fuchsine molecules and functional groups of the adsorbent and π – π electron interactions between phenyl rings of the dye form a multilayer adsorption of fuchsine on to the biosorbent.

Abbreviations

C_i	Initial dye concentration (mg L ⁻¹)
C_f	Final dye concentration of the solution (mg L ⁻¹)
C_s	Saturation concentration of fuchsine and (mg L ⁻¹)
C_e	Dye concentration at equilibrium time (mg L ⁻¹)
q_e	Amounts of fuchsine ions adsorbed per unit mass at equilibrium (mg g ⁻¹)
q_t	Amounts of fuchsine ions adsorbed per unit mass of the sorbent at time t (mg g ⁻¹)
k_1	Pseudo-first order rate constant (min ⁻¹)
k_2	Pseudo-second-order rate constant (g mg ⁻¹ min ⁻¹)
R^1	Liquid film diffusion constant (min ⁻¹)
D_e^1	Effective liquid film diffusion coefficient (cm ² min ⁻¹)
r_0	Radius of the adsorbent particle (cm)
Δr_0	Thickness of the liquid film (cm)
k^1	Equilibrium constant of adsorption

b	Langmuir adsorption coefficient, (L mg ⁻¹)
q_0	Monolayer saturation capacity (mg g ⁻¹)
R_L	The Langmuir adsorption intensity
k_f	Freundlich model constant
n	Adsorption intensity
R	Universal gas constant (8.314 J K ⁻¹ mol ⁻¹)
T	Absolute temperature (K)
E	Mean free energy per molecule of adsorbent (kJ mol ⁻¹)
β	Dubinini–Radushkevich constant (mol ² J ⁻²)
k_a	Langmuir–Freundlich isotherm constant (L mg ⁻¹)
k_{RP}	Redlich–Peterson affinity constant (L mg ⁻¹)
a_{RP}	Redlich–Peterson isotherm constant (mg ⁻¹)
β_1	Index of heterogeneity
V	Volume of fuchsine solution (L)
M	Amount of biomass used (mg)
ΔG	is the Gibbs free energy (kJ mol ⁻¹)
ΔH	Enthalpy change (kJ mol ⁻¹)
ΔS	Entropy change (kJ mol ⁻¹ K ⁻¹)
N_A	Avogadro constant (6.022×10^{23})

Acknowledgements

The authors express their gratitude to the National Research Council of Sri Lanka for their financial support under grant no. NRC 13-087 and to two anonymous reviewers for constructive suggestions.

References

- Z. Carmen and S. Daniela, *Organic Pollutants ten years after the stockholm convention – environmental and analytical update*, 2010, pp. 55–86, DOI: 10.5772/32373.
- B. Zargar, H. Parham and A. Hatamie, *Talanta*, 2009, **77**, 1328–1331.
- C. Cooksey and A. Dronsfield, *Biotech. Histochem.*, 2009, **84**, 179–183.
- S. H. B. Nidadavolu, K. Gudikandula, S. K. Pabba and S. C. Maringanti, *Nat. Sci.*, 2013, **5**, 30–35.
- L. Huang, J. Kong, W. Wang, C. Zhang, S. Niu and B. Gao, *Desalination*, 2012, **286**, 268–276.
- S. S. Hong, *Yonsei Med. J.*, 1974, **15**, 51–57.

- 7 V. K. Gupta, A. Mittal, V. Gajbe and J. Mittal, *J. Colloid Interface Sci.*, 2008, **319**, 30–39.
- 8 G. Crini, *Bioresour. Technol.*, 2006, **97**, 1061–1085.
- 9 R. Rehman, J. Anwar and T. Mahmud, *J. Chem. Soc. Pak.*, 2012, **34**, 460–467.
- 10 K. G. Bhattacharyya and A. Sarma, *Dyes Pigm.*, 2003, **57**, 211–222.
- 11 Y. Guo, S. Yang, W. Fu, J. Qi, R. Li, Z. Wang and H. Xu, *Dyes Pigm.*, 2003, **56**, 219–229.
- 12 A. Shukla, Y.-H. Zhang, P. Dubey, J. Margrave and S. S. Shukla, *J. Hazard. Mater.*, 2002, **95**, 137–152.
- 13 K. Valier, *Ferns of Hawai'i*, University of Hawaii Press, 1995.
- 14 M. D. F. Ellwood, D. T. Jones and W. A. Foster, *Biotropica*, 2002, **34**, 575–583.
- 15 Y. S. Ho and G. McKay, *Adsorpt. Sci. Technol.*, 2002, **20**, 797–815.
- 16 H. Qiu, B.-C. Pan and Q.-X. Zhang, *J. Zhejiang Univ.*, 2009, **10**, 716–724.
- 17 K. Y. Foo and B. H. Hameed, *Chem. Eng. J.*, 2010, **156**, 2–10.
- 18 L.-Z. Huang, G.-M. Zeng, D.-L. Huang, L.-F. Li, C.-Y. Du and L. Zhang, *Environ. Earth Sci.*, 2010, **60**, 1683–1691.
- 19 P. Girods, A. Dufour, V. Fierro, Y. Rogaume, C. Rogaume, A. Zoulalian and A. Celzard, *J. Hazard. Mater.*, 2009, **166**, 491–501.
- 20 E. Turiel, C. Perez-Conde and A. Martin-Esteban, *Analyst*, 2003, **128**, 137–141.
- 21 P. R. Krishna and S. N. Srivastava, *Chem. Eng. J.*, 2009, **146**, 90–97.
- 22 J. C. Y. Ng, W. H. Cheung and G. McKay, *J. Colloid Interface Sci.*, 2002, **255**, 64–74.
- 23 L. Jossens, J. M. Prausnitz, W. Fritz, E. U. Schlünder and A. L. Myers, *Chem. Eng. Sci.*, 1978, **33**, 1097–1106.
- 24 S. Rangabhashiyam, E. Nakkeeran, N. Anu and N. Selvaraju, *Res. Chem. Intermed.*, 2015, **41**, 8405–8424.
- 25 P. T. Hang and G. Brindley, *Clays Clay Miner.*, 1970, **18**, 203–212.
- 26 J. Lützenkirchen, T. Preočanin, D. Kovačević, V. Tomišić, L. Lövgren and N. Kallay, *Croat. Chem. Acta*, 2012, **85**, 391–417.
- 27 N. Priyantha, C. Seneviratne, P. Gunathilake and R. Weerasooriya, *International Journal of Environmental Protection Science*, 2009, **3**, 140–146.
- 28 H. J. Butt, K. Graf and M. Kappl, *Physics and chemistry of interfaces*, Wiley-VCH, Weinheim, 2003.
- 29 J. Coates, in *Encyclopedia of Analytical Chemistry*, ed. R. A. Meyers, John Wiley & Sons Ltd, Chichester, 2000, pp. 10815–10837.
- 30 D. L. Pavia, G. M. Lampman, G. S. Kriz and J. R. Vyvyan, *Spectroscopy*, Cengage Learning India Private Limited, New Delhi, 2009.
- 31 P. K. D. Chathuranga, D. M. R. E. A. Dissanayake, N. Priyantha, S. S. Iqbal and M. C. Mohamed Iqbal, *Biorem. J.*, 2014, **18**, 192–203.
- 32 D. M. R. E. A. Dissanayake, W. M. K. E. H. Wijesinghe, S. S. Iqbal, N. Priyantha and M. C. M. Iqbal, *Ecol. Eng.*, 2016, **88**, 237–241.
- 33 R. S. Bai and T. E. Abraham, *Bioresour. Technol.*, 2003, **87**, 17–26.
- 34 B. Volesky, *Sorption and Biosorption*, BV sorbex, Inc, Montreal, 2003.
- 35 Y. S. Ho, *J. Hazard. Mater.*, 2006, **136**, 681–689.
- 36 K. V. Kumar, *J. Hazard. Mater.*, 2006, **137**, 1538–1544.
- 37 B. I. Olu-Owolabi, P. N. Diagboya and W. C. Ebaddan, *Chem. Eng. J.*, 2012, **195–196**, 270–275.
- 38 K. A. Shroff and V. K. Vaidya, *Chem. Eng. J.*, 2011, **171**, 1234–1245.
- 39 A. Günay, E. Arslankaya and İ. Tosun, *J. Hazard. Mater.*, 2007, **146**, 362–371.
- 40 P. K. Malik, *Dyes Pigm.*, 2003, **56**, 239–249.
- 41 G. P. Jeppu and T. P. Clement, *J. Contam. Hydrol.*, 2012, **129–130**, 46–53.
- 42 S. Rangabhashiyam and N. Selvaraju, *J. Mol. Liq.*, 2015, **209**, 487–497.
- 43 R. Aravindhan, J. R. Rao and B. U. Nair, *J. Hazard. Mater.*, 2007, **142**, 68–76.
- 44 Q.-S. Liu, T. Zheng, P. Wang, J.-P. Jiang and N. Li, *Chem. Eng. J.*, 2010, **157**, 348–356.
- 45 W.-M. Zhang, J.-L. Chen, B.-C. Pan and Q.-X. Zhang, *J. Environ. Sci.*, 2005, **17**, 529–534.
- 46 R. G. Barradas, P. G. Hamilton and B. E. Conway, *J. Phys. Chem.*, 1965, **69**, 3411–3417.
- 47 A. C. M. A. Rocha, I. B. Valentim and F. C. D. Abreu, *European International Journal of Science and Technology*, 2015, **4**, 1–16.
- 48 K. S. Kim, J. Y. Lee, S. J. Lee, T.-K. Ha and D. H. Kim, *J. Am. Chem. Soc.*, 1994, **116**, 7399–7400.
- 49 M. Levitt and M. F. Perutz, *J. Mol. Biol.*, 1988, **201**, 751–754.
- 50 G. Bayramoglu, B. Altintas and M. Y. Arica, *Chem. Eng. J.*, 2009, **152**, 339–346.
- 51 J. Kong, L. Huang, Q. Yue and B. Gao, *Desalin. Water Treat.*, 2013, **52**, 2440–2449.